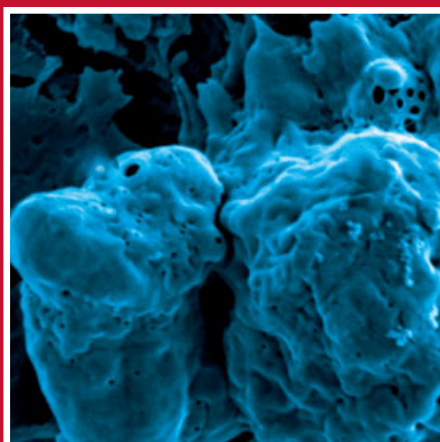
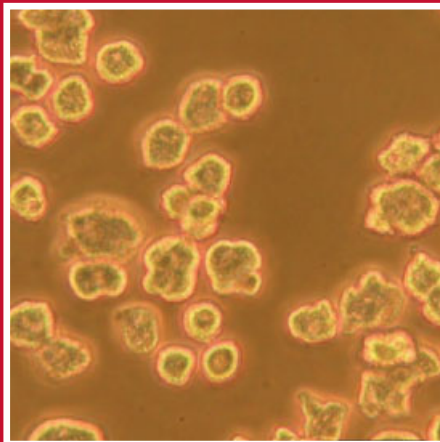


PROTEOMICS

17'11

www.proteomics-journal.com

Animal Proteomics
Bioinformatics
Biomedicine
Cell Biology
Microbiology
Plant Proteomics
Technology



Endorsed as an
Official Journal of



Human Proteome Organisation

 **WILEY-BLACKWELL**

RESEARCH ARTICLE

Lipid bodies in coral–dinoflagellate endosymbiosis: Proteomic and ultrastructural studies

Shao-En Peng^{1,2}, Wan-Nan U. Chen³, Hung-Kai Chen², Chi-Yu Lu⁴, Anderson B. Mayfield², Lee-Shing Fang⁵ and Chii-Shiarng Chen^{1,2,6}

¹ Institute of Marine Biotechnology, National Dong Hwa University, Pingtung, Taiwan

² Taiwan Coral Research Center, National Museum of Marine Biology and Aquarium, Pingtung, Taiwan

³ Department of Biological Science and Technology, I-Shou University, Kaohsiung, Taiwan

⁴ Department of Biochemistry, College of Medicine, Kaohsiung Medical University, Kaohsiung, Taiwan

⁵ Department of Sport, Health and Leisure, Cheng Shiu University, Kaohsiung, Taiwan

⁶ Department of Marine Biotechnology and Resources, National Sun Yat-Sen University, Kaohsiung, Taiwan, ROC

Gastrodermal lipid bodies (LBs) are organelles involved in the regulation of the mutualistic endosymbiosis between reef-building corals and their dinoflagellate endosymbionts (genus *Symbiodinium*). As their molecular composition remains poorly defined, we herein describe the first gastrodermal LB proteome and examine in situ morphology of LBs in order to provide insight into their structure and function. After tissue separation of the tentacles of the stony coral *Euphyllia glabrescens*, buoyant LBs of the gastroderm encompassing a variety of sizes (0.5–4 µm in diameter) were isolated after two cycles of subcellular fractionation via stepwise sucrose gradient ultracentrifugation and detergent washing. The purity of the isolated LBs was demonstrated by their high degree of lipid enrichment and as well as the absence of contaminating proteins of the host cell and *Symbiodinium*. LB-associated proteins were then purified, subjected to SDS-PAGE, and identified by MS using an LC-nano-ESI-MS/MS. A total of 42 proteins were identified within eight functional groups, including metabolism, intracellular trafficking, the stress response/molecular modification and development. Ultrastructural analyses of LBs in situ showed that they exhibit defined morphological characteristics, including a high-electron density resulting from a distinct lipid composition from that of the lipid droplets of mammalian cells. Coral LBs were also characterized by the presence of numerous electron-transparent inclusions of unknown origin and composition. Both proteomic and ultrastructural observations seem to suggest that both *Symbiodinium* and host organelles, such as the ER, are involved in LB biogenesis.

Received: September 1, 2010

Revised: May 10, 2011

Accepted: June 8, 2011

Keywords:

Bleaching / Cell biology / Cnidarian / Lipid droplets / *Symbiodinium* / Symbiont

1 Introduction

Lipid bodies (LBs; also referred to as “lipid droplets”) are organelles found in both eukaryotic and prokaryotic cells, and they have been observed and characterized in bacteria,

plants, invertebrates, and vertebrates [1–3]. Previous studies have indicated that LBs may originate from the endoplasmic reticulum (ER) [4, 5]. Specifically, it has been shown that

Correspondence: Professor Chii-Shiarng Chen, National Museum of Marine Biology and Aquarium, 2 Houwan Road, Checheng, Pingtung 944, Taiwan

E-mail: cchen@nmmba.gov.tw

Fax: +886-8-8825087

Abbreviations: ARF, ADP-ribosylation factor; ASW, artificial seawater; DIC, differential interference contrast; FA, fatty acid; FSW, filtered seawater; LBs, lipid bodies; PAT, Perilipin, Adipose differentiation-related proteins ADRP and TIP47; PC, phosphatidylcholine; PE, phosphatidylethanolamine; RER, rough ER; Rubisco, ribulose-1,5-bisphosphate carboxylase/oxygenase; SER, smooth ER; SGCs, symbiotic gastrodermal cells; TEM, transmission electron microscopy; TG, triglyceride; WE, wax ester

neutral lipids are synthesized between the leaflets of the ER membranes, and mature LBs later bud from the ER to form independent organelles containing a monolayer of phospholipids with a unique fatty acid (FA) composition [6]. The protein composition of LBs has been examined in a variety of cell species, including yeasts, mammalian, and invertebrate cells [5, 7–9]. Characteristically, PAT (Perilipin, Adipose differentiation-related proteins ADRP and TIP47) family proteins are known to specifically associate with LBs in many cell types [2, 10, 11]. Perilipins and ADRP are located on the LB surface and appear to protect the core lipids from hydrolysis by a hormone-sensitive lipase [12]. Overexpression of perilipins results in numerous small lipid droplets [10].

In terms of their cellular function, recent proteomic analyses have demonstrated that LBs not only serve as lipid storage vessels, but are also involved in a dynamic range of biological processes (for review, see [13]). LBs are associated with a multitude of proteins, and their array of cellular functions includes lipid metabolism [14], cholesterol homeostasis [15, 16], membrane trafficking [17, 18], cell signaling [19], transcription, and even regulation of translation [8, 12, 20, 21]. For example, it has been shown that LBs are closely coupled with lipid metabolism in cells [14]. By interacting with cellular microtubules, LBs can rapidly mobilize cellular lipid reservoirs [22]. LBs are also involved in the regulation of differentiation and development [9, 23]. For instance, during the early stages of *Drosophila* embryo growth, LBs serve to store nuclear proteins such as histones [9]. The redistribution of histones from LBs to the nucleus then occurs over the course of development.

The coral-dinoflagellate endosymbiosis is a mutualism in which autotrophic dinoflagellates (genus *Symbiodinium*) reside within the gastrodermal cells of their coral hosts. The molecular mechanisms underlying the regulation of this association remain unclear [24], and the study of coral LBs is still in its infancy. LBs have been postulated to be lipid-based energy reservoirs generated during the endosymbiotic process [25]. Metabolic examinations using radio-labeled acetate and bicarbonate indicated that *Symbiodinium* is the primary contributor of lipids to LBs [26]. However, the cellular function and biogenesis of LBs in this endosymbiosis remain unclear. Ratiometric imaging analyses have documented lipid composition changes in LBs in response to a shift in the symbiotic status of the coral [27]. During stable endosymbiosis in the reef-building coral *Euphyllia glabrescens*, most lipids generated by *Symbiodinium* were transferred to the host coral LBs. However, upon temperature-induced bleaching, whereby the endosymbiosis disintegrates, lipid export to the host LB was diminished, resulting in a decrease in LB abundance, as well as a change in their lipid composition. As the relationship between LBs and endosymbiotic regulation demands further attention [27], LBs were purified from the gastroderm of *E. glabrescens*, and both their protein composition and ultrastructure were characterized.

2 Materials and methods

2.1 Reagents

Iscove's-Modified Dulbecco's Medium (IMDM, Gibco) with NaHCO₃ was purchased from Invitrogen (Carlsbad, CA, USA). The IMDM solution for the treatment of cells was prepared by adding 10% FBS and antibiotics (100 µg/mL streptomycin and 100 units/mL penicillin). All seawater used for the experiment was prepared by filtering through a Vacu-Cap 90 filter (0.2 µm, Gelman Laboratory, Ann Arbor, MI, USA). Artificial seawater (ASW) was also prepared and included 420 mM NaCl, 26 mM MgSO₄, 23 mM MgCl₂, 9 mM KCl, 9 mM CaCl₂, 2 mM NaHCO₃, and 10 mM HEPES (pH 8.2). The osmolarity of all solutions used for the treatment of cells was measured using a Micro-osmometer (Advanced Instruments, Norwood, MA, USA) and was adjusted to 1000 mOsm by addition of NaCl. All chemicals were of analytical grade.

2.2 Coral collection, maintenance, and preparation of amputated tentacles

E. glabrescens colonies (diameter, 7.2–35.8 cm) were collected by SCUBA divers from the inlet of the Third Nuclear Power Plant (21°57.376' N, 120° 45.291' E) at a depth of 3–8 m in Nanwan Bay, Taiwan. Collected colonies were placed in an upright position in a 4-ton outdoor tank with flow-through seawater (at an exchange rate of ~80 L/h) and were maintained under a natural photoperiod with additional air circulation in the husbandry center of the National Museum of Marine Biology and Aquarium (NMMBA). A micro-processor-controlled cooler (HOBO Pendant Temperature/Light Data Logger, UA-002-64, Onset Computer, Bourne, MA, USA) was linked to the tank and the temperature was maintained at 26.5 ± 1°C. Amputated tentacles were obtained from polyps of *E. glabrescens* colonies using curved surgical scissors and then transferred to the laboratory and washed with filtered seawater (FSW) for further use.

2.3 Preparation of isolated symbiotic gastrodermal cells

Isolated symbiotic gastrodermal cells (SGCs) were obtained from amputated tentacles which were turned inside-out according to a previously-published procedure [27, 28]. Cells were then suspended in FSW at a final concentration of ~1–2 × 10⁶/mL and the intactness of their plasma membranes examined [27, 28].

2.4 Fluorescent labeling of LBs and the ER in SGCs and gastrodermal tissues

Cryo-sections were obtained by an improved method in order to achieve better resolution of tentacle tissues [29].

Briefly, amputated tentacles of *E. glabrescens* were rinsed with FSW and anesthetized with 7% MgCl₂ for 10 min. They were then fixed in 3.6% paraformaldehyde and 5% sucrose in PBS for 1 h at room temperature and subsequently incubated with PBS containing 5% sucrose, 15.7 μM Nile red (9-diethylamino-5H-benzo[α]phenoxazine-5-one, Sigma-Aldrich, St. Louis, MO, USA; [30]), and 16 μM Hoechst 33342 (Invitrogen) for 10 min to label LBs and the cell nuclei, respectively.

Cryoprotection was achieved by infiltrating the tentacle with sucrose of increasing concentrations. Samples were incubated with 5 and 20% sucrose in PBS in volume ratios of 2:1, 1:1, and 1:2 in series (each step for 30 min). Then, sucrose-infiltrated tentacles were embedded with a 20% sucrose: OCT compound (2:1 in volume ratio; OCT compound: Jung tissue freezing medium from Leica) for 20 min at −30°C. The tentacles were then sectioned at a thickness of 3 μm using a Leica CM 1850 Cryostat (Leica Microsystems, Nussloch, Heidelberg, Germany). The sections were placed onto polylysine precoated slides (Polyscience, Menzel), washed with ddH₂O three times, and mounted using ProLong Gold[®] antifade reagent (Invitrogen) for microscopy.

SGCs were first loaded onto polylysine pre-coated slides and incubated for 1 h at room temperature. They were then fixed with 3.6% paraformaldehyde in PBS for 1 h at room temperature, washed three times with PBS, and finally stained with 15.7 μM Nile red in PBS for 10 min.

Labeling of the ER in the live gastroderm was performed as follows. A stock ER-specific probe, ER-Tracker[™] Green (glibenclamide BODIPY[®] FL; Invitrogen) was prepared at 1 mM in DMSO and stored at −20°C for use. Amputated tentacles were incubated in ASW containing 4 μM ER-Tracker[™] Green (final DMSO concentration, <1%) at room temperature for 1 h. Nonbound probe was removed by washing with FSW. Taking advantage of the elastic properties of the epiderm, the pure gastroderm was then obtained as described previously [27]. The isolated gastroderm was then placed onto a concave slide and covered with a 22 × 22-mm coverslip for observation with confocal microscopy.

2.5 LB purification

An outline of the procedure for LB purification is shown in Fig. 1. The procedure included three steps; (a) LB isolation, (b) purity assessment, and (c) 1-D SDS-PAGE and MS.

(a) *LB isolation.* Eighty tentacles (stretched length, ~3 cm) from *E. glabrescens* were collected as above. After rinsing with FSW, tentacle tips were removed using microscissors (Spring Type, AESCULAP, Center Valley PA, USA) to decrease the presence of nematocytes and prevent their interference during the isolation process. The gastroderm was then separated using ASW containing 3% *N*-acetylcysteine (pH 8.2) as described previously

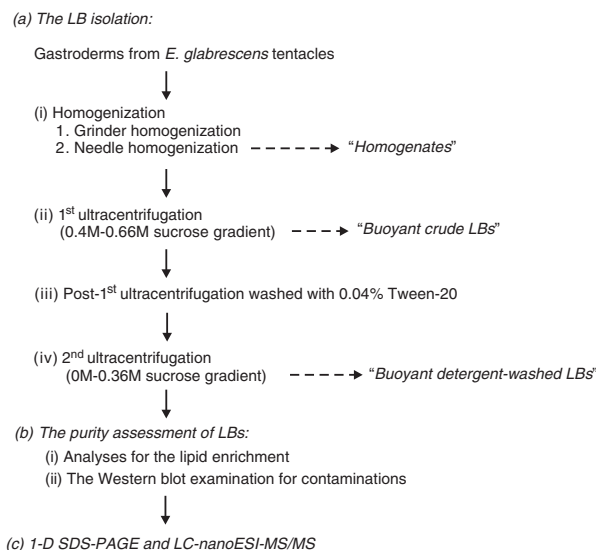


Figure 1. An outline of the procedure for LB purification and proteomic analysis.

[31]. After an incubation in 2 mL of ASW containing 1 × complete protease inhibitor cocktail (25 × stock solution in 2 mL ddH₂O, Cat. 11697498001; Roche, Madison, WI, USA), the total gastrodermal layers were homogenized on ice with ten passes of a 7-mL glass tissue grinder (Kimble/Kontes, Vineland, NJ, USA). The crude homogenate was then passed through a syringe (23G × 1 (1/4)", Top Surgical, Taiwan) 15 times. This resulted in the "Homogenates" fraction in which gastrodermal cells were thoroughly broken to release intracellular LBs, yet not so thoroughly homogenized as to destroy *Symbiodinium* cells (Fig. 1).

For the first stepwise sucrose gradient ultracentrifugation (0.4–0.66 M top-bottom), the resulting "Homogenates" (~1.8 mL) were mixed with cold 1.2 M sucrose (2.2 mL in PBS plus 1 × protease inhibitor cocktail, pH 7.5) in a 12-mL ultracentrifugation tube (UltraClean tube, Beckman Coulter, Brea, CA, USA). The top of the solution was overlaid with cold 0.4 M sucrose (6 mL in PBS plus 1 × protease inhibitor cocktail, pH 7.5) and spun at 150 000 × g (4°C) for 30 min using a swing rotor (SW-41, Optima L-100 XP Ultracentrifuge, Beckman Coulter). Afterward, fractions were collected every 2 mL from the top to the bottom of the centrifugation tube. The top layer containing LBs was deemed the "Buoyant crude LBs" fraction (1.6 mL, Fig. 1). Other collected fractions (i.e. fractions 1–2 to 1–5, from the top to the bottom of the centrifuge tube) were kept for lipid and protein analyses. The "Buoyant crude LBs" were then incubated with cold 0.33 M sucrose (2.4 mL in PBS plus 1 × protease inhibitor cocktail) containing Tween-20 (final concentration, 0.04%; Sigma-Aldrich) at 4°C for

10 min to remove cellular materials attached to the outside of the LBs (the “post-1st ultracentrifugation washed with 0.04% Tween-20” in Fig. 1).

For the second stepwise sucrose gradient ultracentrifugation (0–0.36 M top-bottom), the Tween-20-washed homogenate (4 mL) from the first ultracentrifugation was transferred to a new ultracentrifugation tube. Then, the top was overlaid with 6 mL of cold PBS (plus 1 × protease inhibitor cocktail) and spun at 150 000 × *g* at 4 °C for 60 min. Afterwards ten fractions (1 mL each) were collected from the top to the bottom. The top layer containing LBs was deemed the “Buoyant detergent-washed LBs” (Fig. 1).

(b) *Purity assessment of LBs.* To evaluate the LB purity in the collected fractions, analyses were conducted to attempt to demonstrate both a high degree of lipid enrichment (verified with TLC) and an absence of contamination of host and *Symbiodinium* proteins (verified by Western blotting).

(i) *Lipid analyses.* Lipid contents of collected fractions were extracted by the Bligh and Dyer procedure [32] followed by TLC using silica-coated TLC plates (20 × 20 cm², F₂₅₄, Analtech, Germany), with six repetitions for each collected fraction. Chromatography was sequentially conducted by two solvent systems modified from the previous reports [33, 34]. Briefly, TLC was first developed to the *R_f* = 0.5 position in chloroform: ethanol: H₂O: triethylamine (35:35:7:35 v/v/v/v). The plate was air-dried and then developed to the top (*R_f* = 1) in hexane:diethyl ether: acetic acid (70:30:1 v/v/v). Lipid standards for wax esters (WE), sterols, triglycerides (TGs), FAs, and phospholipids were composed of palmityl palmitate, cholesterol, tripalmitin, palmitic acid, phosphatidylethanolamine (PE), phosphatidylcholine, and lyso-phosphatidylcholine, respectively (from Sigma-Aldrich or Matreya, PA, USA). The lipid visualization on TLC plates was performed by staining with 0.03% Coomassie blue R 250 (from Sigma; in 20% methanol containing 0.5% acetic acid) [35]. Concentrations of individual lipid species were then quantified using the Metamorph Image Processing system (Molecular Devices, Toronto, Canada), based on the calibration curves of individual lipid standards corun on the same TLC plate.

(ii) *Western blot examination.* LBs were delipidated according to the procedure described by Mastro and Hall [36]. Briefly, the “delipidation solution” (tributyl phosphate: acetone:methanol, 1:12:1 v/v/v) was added to the collected fractions at a 14:1 volume ratio on ice, followed by incubation at –20 °C overnight. Precipitated proteins were then collected (3202 × *g* for 15 min at 4 °C), washed sequentially with ice-cold methanol, tributyl phosphate, and acetone (30 min at 4 °C each), and spin vacuum-dried at room temperature for 10–20 min. The precipitated proteins were then resuspended in 1 × sample buffer (62.5 mM Tris-HCl, pH 6.8, 2% SDS, 10% glycerol,

10 mM DTT) and quantified with the 2-D Quant Kit (Cat. 80-6483-56, GE Healthcare, Piscataway, NJ, USA). Ten microgram (10 μg) of each protein sample was subjected to 12% SDS-PAGE using a Bio-Rad electrophoresis unit (Mini PROTEAN[®] 3 cell) [37]. Afterward, the SDS-PAGE gel was equilibrated in Towbin buffer (25 mM Tris, 192 mM glycine, 20% MeOH, 0.1% SDS, pH 8.0; [38]) and then blotted onto PVDF membranes (immobilon-PSQ 0.45 μm; Millipore) using the Bio-Rad Transblot[®] apparatus (100 V for 2 h at 4 °C). The membranes were incubated in blocking buffer (5% skim milk, 0.1% Tween-20, 100 mM Tris, 150 mM NaCl, pH 7.6) at room temperature for 1 h, followed by incubation with a mAb cocktail of rabbit anti-ribulose-1,5-bisphosphate carboxylase/oxygenase (Rubisco) large subunit (1:2000 dilution; Cat. AS0 037, Agrisera, Vannas, Sweden), mouse anti-actin (1:4000 dilution; Cat. MAB1501, Millipore) and mouse anti-ADP-ribosylation factor (ARF) (1:500 dilution; Cat. Ab2806, Abcam, Cambridge, MA, USA) in TBS-T buffer (0.1% Tween-20, 100 mM Tris, 150 mM NaCl, pH 7.6) at 4 °C overnight. The membranes were then washed five times with TBS-T for 10 min and incubated with a HRP-conjugated goat anti-rabbit and anti-mouse IgGs (Millipore) in TBS-T buffer (1:500 dilution). The membranes were subsequently washed and the resulting proteins visualized using SuperSignal West Pico Chemiluminescent substrate kits (Cat. 34080, Thermo Fisher Scientific, Waltham, MA, USA) according to the manufacturer’s recommendations.

2.6 Protein identification by LC-nano-ESI-MS/MS analysis

Proteins separated on the SDS-PAGE gels were stained with Sypro[®] Ruby according to the manufacturer’s instructions (Invitrogen). Briefly, the gels were fixed twice with 50% methanol and 7% acetic acid in ddH₂O for 15 min, stained overnight in 400 mL Sypro Ruby solution, then washed in 10% methanol and 7% acetic acid in ddH₂O for 30 min. After a final wash in ddH₂O for 20 min, a fluorescent image scanner (Typhoon TRIO, GE Healthcare) was used for protein visualization.

Prominent protein bands on the gel were manually excised and cut into pieces for MS analysis according to a published procedure [24]. Briefly, the gel pieces were rehydrated with 50 mM DTT in 25 mM ammonium bicarbonate (pH 8.5) at 37 °C for 1 h, and subsequently alkylated with 100 mM iodoacetamide in 25 mM ammonium bicarbonate (pH 8.5) in the dark at room temperature for 1 h. They were then washed twice with ammonium bicarbonate buffer (pH 8.5) containing 50% ACN (50 mM ammonium bicarbonate: ACN, 1:1 v/v), dehydrated with 100% ACN for 5 min, vacuum-dried and digested in 15 μL 25 mM ammonium bicarbonate (pH 8.5) containing 150 ng modified trypsin (sequencing-grade from Promega, Madison, WI, USA) at

37°C for 16 h. Following digestion, tryptic peptides were extracted twice with 50 μ L ACN/TFA/ddH₂O (50:5:45 v/v/v) for 15 min each time with moderate sonication, and the extracted solutions were then pooled and thoroughly evaporated under a vacuum. The samples were subsequently dissolved in formic acid/ACN/ddH₂O (0.1:50:49.9 v/v/v) and analyzed by LC-nano-ESI-MS/MS.

MS/MS ion searches were performed on the processed spectra against the NCBI nonredundant database using the MASCOT search program (www.matrixscience.com). The mass tolerance parameter was 20 ppm, the MS/MS ion mass tolerance was 1 Da, and up to one missed cleavage was allowed. Variable modifications considered were methionine oxidation and cysteine carboxyamidomethylation. Positive identification of proteins was confirmed by observation of at least one of the following criteria: (i) the total number of matched peptides (mps) is more than 2, or (ii) the mps equals 2 with two different matched peptides, or (iii) the mps equals 2 resulting from the same matched peptide, but with a MOWSE score at least 20 higher than the significance threshold, which indicates identity or extensive homology ($p < 0.05$).

2.7 Fluorescence and transmission electron microscopy

Differential interference contrast (DIC) microscopy and fluorescence microscopy were performed using either an inverted microscope (Axiocvert 200 M, Zeiss, Oberkochen, Germany) or an upright microscope (Axioskop 2 plus, Zeiss) equipped with a Plan-Neofluar (1.3 N.A.) objective and epifluorescent optics for various fluorophores, including cy3, fluorescein and DAPI. CCD cameras (Quantix or CoolSNAP-Procf, Photometrics, AR, USA) were employed to obtain the microscopic images using suitable exposures. Confocal microscopy was performed using an LSM 510 confocal microscope (Zeiss).

To investigate the in situ ultrastructure of LBs in the gastroderm, tentacles were fixed in 2.5% glutaraldehyde/2% paraformaldehyde/100 mM sodium phosphate containing 5% sucrose (pH 7.3) for 2.5 h at 4°C, then washed with 100 mM sodium phosphate at 4°C. They were then post-fixed in 1% OsO₄ in 50 mM sodium phosphate (pH 7.3) for 1 h at 4°C. The tissue blocks were washed with water, dehydrated with increasing ethanol concentrations (50, 70, 80, 90, 95, and 100%), and embedded in Spurr's resin (Electron Microscopy Sciences, Hatfield, PA, USA). Sections were then post-stained in 2.5% uranyl acetate in methanol and 0.4% lead citrate, deposited onto copper grids and air-dried. Samples were imaged using a JEM-1400 transmission electron microscope (JEOL, Japan).

2.8 Statistical analysis

All statistical analyses were performed using SigmaStat 3.5 (Systat software, Chicago, IL, USA). The results were expressed as mean \pm SD (standard deviation of the mean).

3 Results and discussion

Lipid droplets have emerged as a pivotal organelle in eukaryotic cells and are involved in various functions, including lipid metabolism [14], membrane trafficking [17, 18], cell signaling [19], and regulation of transcription and translation [8, 12, 20, 21]. Nevertheless, the study of lipid droplets in mutualisms between anthozoan corals and the dinoflagellate endosymbionts has been neglected since they were first identified in the 1980s [25]. Examination using fluorescent ratiometric imaging of *E. glabrescens* showed that there were several unique features of gastrodermal LBs, including (i) they can be identified by the lipid probe Nile red, (ii) their exclusive presence in SGCs, and (iii) their biogenesis and lipid composition being dependent on symbiotic status [27]. These findings clearly demonstrated their pivotal role in regulation of endosymbiosis.

Herein, the Nile red staining of tentacle tissues revealed that the LBs were specifically located in the gastrodermal tissue layer in a highly concentrated region close to the lumen (Fig. 2A, C). Under DIC microscopy, LBs were observed as opaque globules with an average size of $\sim 3.47 \mu\text{m}$ (arrows in Fig. 2B and D). Due to their high lipid content, LBs were specifically labeled by the lipophilic probe Nile red (Fig. 2D). Their cellular location was further examined in SGCs isolated from the gastrodermal layer (Fig. 2E and F). A representative LB within a SGC containing four *Symbiodinium* cells is shown in Fig. 2E. It used to locate in the peri-nucleus region (filled arrows in Fig. 2E and F denote the nucleus of the SGC). SGCs with multiple LBs were also observed periodically (Fig. 5A). As both the molecular composition and the cellular function of LBs remain a mystery, LB-associated proteins and LB ultrastructure in the gastroderm were investigated.

3.1 LB purification

To date, there have been no reports of successful LB purification from a cnidarian-dinoflagellate association. "Extra-algal lipid droplets" have been isolated from the sea anemone *Condylactis gigantea* and the hermatypic coral *Stylophora pistillata* for radio-labeled lipid examinations ([25, 39], respectively). However, there was no analytical information regarding the purity of the isolated droplets. In fact, as shown by a later report, the identification of these "extra-algal droplets" was questionable, as they might have simply been host nuclei [40].

Moreover, although the high lipid content and consequent low buoyant density of LBs enables rapid isolation by floatation, nonspecific residue from the cell lysate may result in the identification of contaminated proteins [13, 41]. Proteomic analysis is a versatile tool to investigate protein expression during various physiological and developmental processes [42]. However, proteins present in low concentrations in samples containing multiple tissues may not be

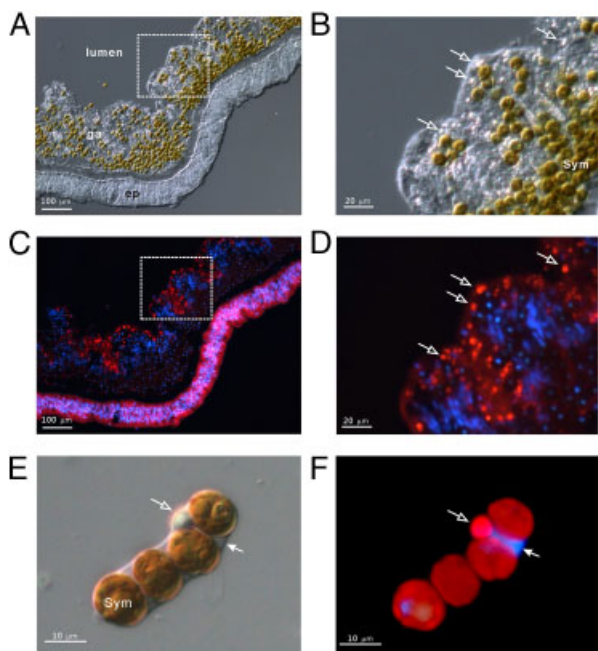


Figure 2. Distribution of LBs in SGCs in *E. glabrescens*. The distribution of the LB population in cryosections of coral tentacles was examined by DIC and fluorescence microscopy. (A) DIC image of a tentacle section showing LBs distributed specifically in the gastroderm (ga). ep, epiderm. (B) Magnified inset of (A) showing the LB distribution (blank arrows). (C) Nile red staining of the LBs of (A) under a fluorescent microscope. The blue fluorescence indicates nuclei stained with Hoechst 33342. (D) The same magnified inset as shown in (B) under a fluorescent microscope. (E and F) DIC and Nile red staining images of a SGC isolated from the gastroderm, which show the distribution of a LB (blank arrow) and the nucleus of the SGC (filled arrow). Sym, *Symbiodinium*.

detected. This is particularly true in attempts to investigate the expression of gastrodermal proteins involved in marine endosymbiosis, as interference may be caused by proteins from the epidermal tissue layer [31]. Hence, the gastroderm was first separated from the epiderm of the coral *E. glabrescens* by treatment with *N*-acetylcysteine (NAC), which was previously shown to have negligible impact on protein integrity [31].

After tissue layer separation, a procedure was developed to purify LBs directly from the SGCs by two cycles of subcellular fractionation and detergent washes (Fig. 1). This process starts with LB isolation from the gastroderm; first, homogenization is achieved through a glass tissue grinder followed by a syringe to break host gastrodermal cells (but not *Symbiodinium*) and release only host LBs. This process greatly decreased the contamination of *Symbiodinium* proteins (data not shown).

The isolated LBs with low buoyant density were then harvested after two cycles of stepwise sucrose gradient ultracentrifugation and detergent washes with Tween-20. Because of the viscous nature of the homogenates, due to

the mucus secretion from coral tissues during the homogenization, one single cycle of stepwise sucrose gradient ultracentrifugation (i.e. 0–0.66 M, from top to the bottom) resulted in unsatisfactory fractionations. Here, the LB population could not be concentrated to the floating layer (data not shown). Mucus has been reported to bind with the lipid vesicles [43], and may thus interfere with the buoyant density of LBs. As a consequence, the ultracentrifugation fractionation with two cycles for stepwise sucrose gradient (first, 0.4–0.66 M; second, 0–0.36 M) was developed to remove mucus efficiently and for the better LB recovery.

The purity of isolated LBs was then demonstrated by their high lipid content relative to that of whole tissue extracts and the lack of contamination of marker proteins from the host coral and *Symbiodinium*. The major characteristic of lipid droplets in eukaryotic cells is their high concentration of neutral lipid triglycerides (TGs) (for review,[44]). Besides, cholesteryl ester, cholesterol (or sterols) and wax ester (WE) have also been reported to be enriched in lipid droplets of mammals [10, 41, 44], plants [44], and the Cnidaria [26, 27, 45]. As there is currently no protein marker for coral LBs, the enrichments of these lipids in the fractionated samples compared with those of the tissue homogenate were used as the first assessment for LB purity. First, as shown in Fig. 3A, there were both neutral and polar lipids detected in LBs, including WEs, TGs, sterols, FAs, and three phospholipids (PE, phosphatidylcholine [PC], and lysophosphatidylcholine [lysoPC]). It was evident that lipid levels in the “Buoyant detergent-washed LBs” fraction after the 0.04% Tween-20 wash and the second sucrose gradient ultracentrifugation (0–0.36 M, top to bottom) were greatly enriched in comparison to those of the “Buoyant crude LBs” fraction after the first sucrose gradient ultracentrifugation (0.4–0.66 M, top to bottom). With the exception of FA, all of the six lipid species were considerably enriched in the “Buoyant detergent-washed LBs.” Specifically, in comparison to the lipid concentrations in the “Homogenate,” there were 36-fold, 26-fold, and 119-fold higher concentrations of WE (7.31 ± 0.55 versus 0.20 ± 0.01 $\mu\text{g}/\mu\text{g}/\text{protein}$), TG (87.21 ± 10.20 versus 3.38 ± 0.04 $\mu\text{g}/\mu\text{g}/\text{protein}$), and sterols (6.92 ± 0.87 versus 0.06 ± 0.01 $\mu\text{g}/\mu\text{g}/\text{protein}$), respectively, in the “Buoyant detergent-washed LBs” (Table 1).

The purity of LBs was further assessed by Western blot using antibodies against two selected host proteins, the small GTPase ADP-ribosylation factor (ARF) and actin, and one *Symbiodinium* protein, ribulose-1,5-bisphosphate carboxylase/oxygenase (Rubisco). The ARFs were selected as the marker for the contamination from the host cell because of its broad subcellular distribution. Depending on different species (ARF1–ARF6) and activities, ARFs distribute in the plasma membrane, cytosol, the vesicular system, and ER–Golgi, [46, 47]. The anti-ARF mAb used in this study recognizes ARF1, ARF3, ARF5, and ARF6 according to the manufacturer’s direction and a published report [48]. The host actins with a molecular weight of ~ 43 kDa were selected as additional host marker proteins as described in a

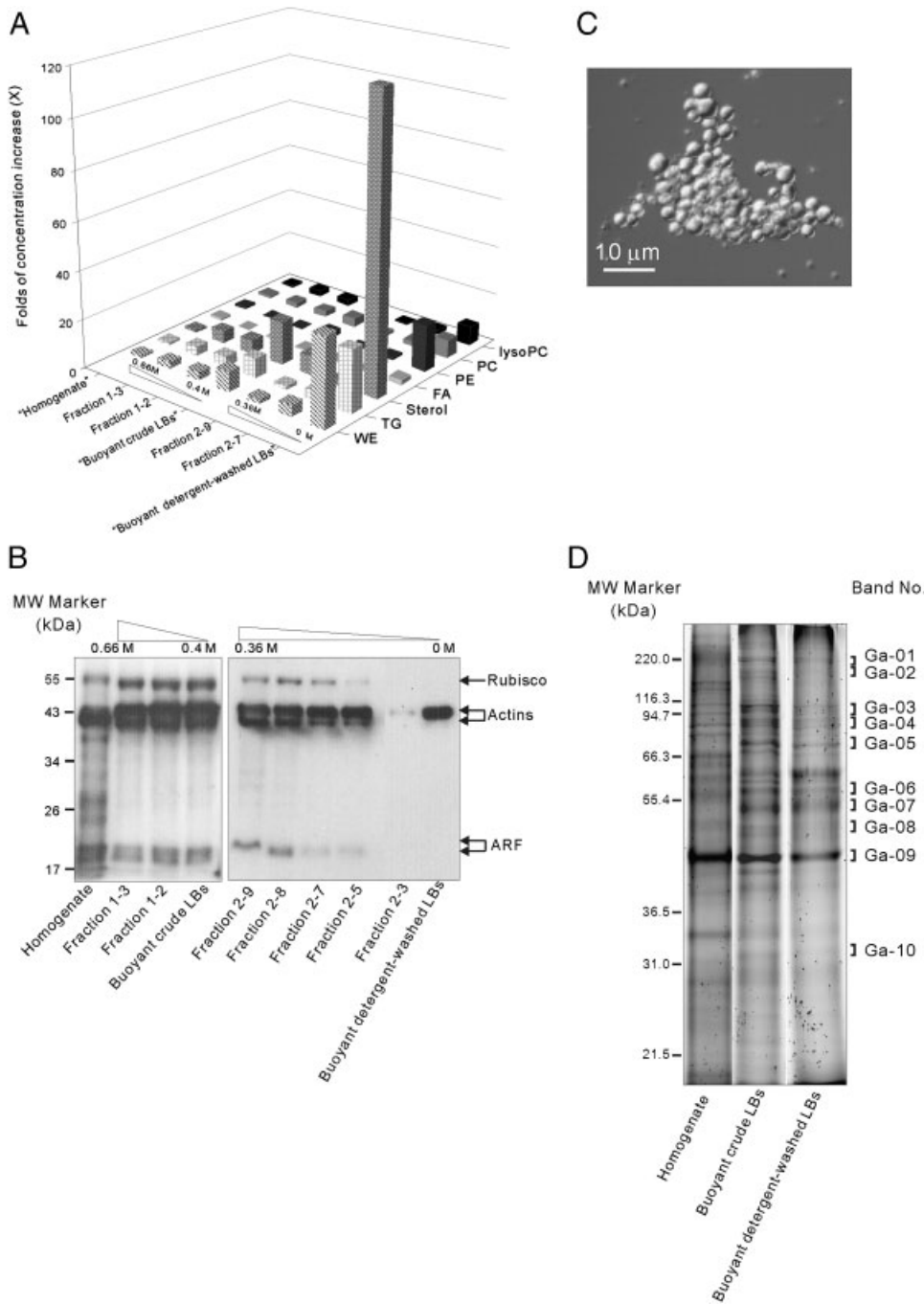


Figure 3. The purity and protein profile of purified LBs during the subcellular fractionation. LBs were isolated and purified as shown in Fig. 1. (A) Fold increases in the concentration of lipids in collected fractions during the two cycles of subcellular fractionation. (B) Western blot examination of collected fractions for the determination of potential contamination from *Symbiodinium* (Rubisco) and the host cells (actins and ARF). The purified LBs (i.e. the "Buoyant detergent-washed LBs") only contained a single actin protein. (C) A representative DIC image of purified LBs in the "Buoyant detergent-washed LBs" fraction. (D) The protein profile of "Buoyant detergent-washed LBs" was resolved by SDS-PAGE and compared with that of the "Homogenate" and "Buoyant crude LBs." The protein profile of the "Buoyant detergent-washed LBs" was reproducible in at least three different LB purifications, and a total of ten proteins bands (Ga-1 to Ga-10) were removed for proteomic analysis.

previous report [24]. As shown in Fig. 3B, the "Homogenate" and all fractions after the first sucrose gradient ultracentrifugation, including the "Buoyant crude LBs" fraction, contained both host and *Symbiodinium* marker proteins, indicating the presence of contamination from the host and *Symbiodinium*. The Western blot showed that the antibodies recognized Rubisco, actin, and ARF at molecular weights of ~55, ~43 (a doublet), and ~21 kDa (a doublet), respectively. The "Buoyant crude LBs" fraction was then

subjected to 0.04% Tween-20 wash, followed by a second sucrose gradient ultracentrifugation. As shown, Rubisco and ARF were removed in the "Buoyant detergent-washed LBs" fraction. Interestingly, the actin doublet that was originally present in the "Buoyant crude LBs" was resolved after the second ultracentrifugation. The upper actin singlet was still present in the purified LBs, indicating the presence of a specific type of actin associated with LBs (discussed in greater detail below). Furthermore, the contaminated ARF

Table 1. Lipid contents of homogenates and buoyant fractions containing LBs after two cycles of subcellular fractionation

Lipids ^{a)}	Homogenate		"Buoyant crude LBs"		"Buoyant detergent-washed LBs"		
	($\mu\text{g}/\mu\text{g protein}$) ^{b)}	[folds] ^{c)}	($\mu\text{g}/\mu\text{g protein}$)	[folds]	($\mu\text{g}/\mu\text{g protein}$)	[folds]	(molecule no./ $\mu\text{g protein}$) ^{d)}
WE	0.20±0.01	[1 ×]	1.68±0.09	[8.39 ×]	7.31±0.55	[36.49 ×]	9.15 × 10 ¹⁵
TG	3.38±0.04	[1 ×]	26.61±1.95	[7.87 ×]	87.21±10.2	[25.78 ×]	6.51 × 10 ¹⁶
Sterol	0.06±0.01	[1 ×]	1.02±0.04	[17.69 ×]	6.92±0.87	[119.40 ×]	1.08 × 10 ¹⁶
FA	0.53±0.05	[1 ×]	0.27±0.05	[0.51 ×]	1.09±0.00	[2.08 ×]	2.56 × 10 ¹⁵
PE	0.02±0.00	[1 ×]	0.05±0.00	[2.71 ×]	0.33±0.00	[18.95 ×]	2.67 × 10 ¹⁴
PC	0.40±0.02	[1 ×]	1.37±0.18	[3.45 ×]	2.93±0.46	[7.51 ×]	2.32 × 10 ¹⁵
Lyso PC	0.20±0.01	[1 ×]	0.58±0.04	[2.89 ×]	1.58±0.70	[7.88 ×]	3.18 × 10 ¹⁵

a) Analyses of lipids by TLC using commercial lipids as standards (Section 2), including WE (Palmityl palmitate, MW. 480.85), TG (Tripalmitin, MW. 807.34), Sterol (Cholesterol, MW. 386.65), FA (Palmitic acid, MW. 256.42), PE (PE, MW. 744.05), PC (PC, MW. 760.09), Lyso PC (Lysophosphatidylcholine, MW. 299.26).

b) Lipid contents are expressed as lipid/protein ($\mu\text{g}/\mu\text{g}$); Data are presented as mean ± SD ($n = 6$).

c) Folds of concentration increases compared with the lipid concentration of homogenates.

d) Molecule number per microgram protein, was calculated based on the lipid concentration, molecular weight of individual lipid and Avogadro's number.

doublet was also resolved into different fractions, and then completely removed from the purified LBs in the "Buoyant detergent-washed LBs" fraction. Comparison studies showed that ARF still could be removed from the buoyant LB fraction after the second sucrose gradient ultracentrifugation without the Tween-20 washing (data not shown). Nevertheless, without the Tween-20 washing, contaminated proteins from the symbiont chloroplast, such as Rubisco and PCP (peridinin-chlorophyll *a*-binding protein), could not be removed. This indicates that the detergent wash and second ultracentrifugation are required to improve the purity of LBs. It also clearly showed that the ARF was not a LB-associated protein, and further validated its use as the host protein marker to assess the LB purity.

Several detergents, including SDS, Triton X-100, and Tween-20, were tested for their ability to remove cellular debris from the LBs while demonstrating minimal impact on LB integrity. The ionic detergent SDS at concentrations of 0.04–0.1% readily destroyed LBs. The nonionic detergent Triton X-100 at similar concentrations tended to induce size increases in LBs. Finally, Tween-20 at a concentration (0.04%) lower than its CMC (~0.06% at 21°C; [49]) was shown to be the preferred detergent for LB washes. The 4°C-wash might further increase the CMC of Tween-20 [50] and prevent solubilization of LB-associated proteins by 0.04% Tween-20, as there was no observable change in LB size after Tween-20 washing (data not shown). The morphology of the purified LBs in the "Buoyant detergent-washed LBs" was remarkably stable, and they remained isolated with no noticeable changes in size during the purification process (Fig. 3C). Furthermore, they did not aggregate or coalesce, even after prolonged storage at –80°C or following freeze–thawing. It is possible, then, that proteins on the LB surface act to prevent cell fusion, as has been shown in lipid droplets of other eukaryotes [51–53].

3.2 Analysis of LB-associated proteins by SDS-PAGE and MS

After SDS-PAGE, protein profiles of the gastrodermal "Homogenates," the "Buoyant crude LBs" and purified "Buoyant detergent-washed LBs" were compared (Fig. 3D). Ten LB-associated protein bands in the purified LBs (Ga-01 to Ga-10 in the "Buoyant detergent-washed LBs") were removed and analyzed by MS, and 42 LB-associated proteins were identified (Table 2). These LB-associated proteins were heterogeneous in origin and function, and, based on NCBI homology searches, 85.7% (36 of the 42 proteins) appeared to be of animal origin, with 33.3% (12/36) being most similar to published cnidarian protein sequences. It was assumed that the proteins with the highest degree of similarity to animals were of host origin. On the other hand, only 11.9% (5/42) and 2.3% (1/42) were presumed to be of bacterial and plant origin, respectively, and the latter was assumed to be from *Symbiodinium*.

In addition to the heterogeneous nature of their origin, the identified proteins are involved in a variety of cellular functions (Fig. 4), including energy metabolism (21%), cytoskeleton dynamics and intracellular trafficking (21%), protein folding (17%), DNA repair and metabolism (10%), lipid metabolism (7%), protein biosynthesis and metabolism (7%), transport (7%), and assorted other roles (10%). This protein composition is distinct from that of lipid droplets in other eukaryotic cells. Among the 42 proteins identified, 57.1% (24 proteins) have been identified as lipid droplet-associated proteins in other cell types (Table 2 and references cited therein), whereas 42.9% (18 proteins) were unique to LBs of coral.

Among the various structural proteins identified in the lipid droplets of other eukaryotic cells, the PAT protein family (Perilipin, ADRP, and TIP47) has been shown to be most abundant and has become a protein marker for lipid droplets [2]. PAT proteins are responsible for droplet

Table 2. Identification of gastrodemic LB proteins

Protein name	Species/Taxonomy	Band no.	GI no.	MS/mps(p) ^{a)}	Sequence coverage (%)	Predicted MW (kDa)	Observed MW (kDa)	Found with LBs in other organisms	Reference(s)
Lipid metabolism									
Hypothetical protein BRAFLDRAFT_206306 (Phospholipase D)	<i>Branchiostoma floridae</i> (Florida lancelet)/Chordata	Ga-07	261289723	75/3(1)	1	109.31	54.62		
Predicted protein (S-adenosyl-L-homocysteine hydrolase)	<i>Nematostella vectensis</i> (sea anemone)/Cnidaria	Ga-08	156401481	80/3(2)	4	47.900	51.00	Yes	[59]
Unnamed protein product (acetyl-CoA acetyltransferases)	<i>Tetraodon nigroviridis</i> (pufferfish)/Vertebrata	Ga-08	47207032	83/2(2)	3	49.242	51.00	Yes	[9]
Energy metabolism									
ATP synthesis									
Mitochondrial ATP synthase subunit α precursor	<i>Litopenaeus vannamei</i> (shrimp)/Crustacea	Ga-06	288816877	411/17(11)	24	59.188	58.20	Yes	[52]
NAD(P) transhydrogenase subunit	<i>N. vectensis</i> (sea anemone)/Cnidaria	Ga-03	156349276	86/2(2)	1	105.365	104.60		
Predicted protein (F1 ATP synthase β subunit)	<i>N. vectensis</i> (sea anemone)/Cnidaria	Ga-07	156364605	722/21(10)	32	44.812	54.62	Yes	[52]
Predicted protein [NADH dehydrogenase (ubiquinone) Fe-S protein]	<i>N. vectensis</i> (sea anemone)/Cnidaria	Ga-05	156406590	49/2(2)	3	79.919	75.40	Yes	[52]
Glycolysis									
Enolase	<i>Polyxenus fasciculatus</i> (millipede)/Arthropoda	Ga-07	8101740	107/4(1)	5	41.408	54.62	Yes	[52]
Fructose 1,6-bisphosphate aldolase	<i>Antheraea yamamai</i> (Japanese oak silkworm)/Insecta	Ga-07	45330818	115/2(2)	7	39.684	54.62		
Glyceraldehyde-3-phosphate dehydrogenase	<i>Limnitis reducta</i> (butterfly)/Insecta	Ga-07	161088548	148/2(2)	16	24.179	54.62	Yes	[5, 8, 20]
TCA cycle									
Citrate synthase	<i>Aedes aegypti</i> (mosquito)/Insecta	Ga-07	157130536	149/5(3)	7	51.608	54.62		
Predicted: similar to isocitrate dehydrogenase	<i>Tribolium castaneum</i> (red flour beetle)/Insecta	Ga-07	189234287	187/8(3)	10	39.004	54.62		
Molecular chaperone									
78 kDa glucose-regulated protein (GRP78/BiP)	<i>Culex quinquefasciatus</i> (mosquito)/Insecta	Ga-05	170034715	435/15(7)	15	72.263	75.40	Yes	[5, 12, 15, 17, 19]
Predicted protein (molecular chaperone DnaK)	<i>N. vectensis</i> (sea anemone)/Cnidaria	Ga-05	156402816	71/2(2)	5	69.611	75.40	Yes	[12]
Predicted protein (heat shock protein 70 kDa)	<i>N. vectensis</i> (sea anemone)/Cnidaria	Ga-05	156361178	81/7(6)	12	73.822	75.40	Yes	[5, 12, 15, 17, 19]
Predicted protein (heat shock protein 90 kDa)	<i>N. vectensis</i> (sea anemone)/Cnidaria	Ga-03	156396452	235/5(4)	5	97.726	104.60	Yes	[19, 64]
Similar to heat shock protein 60 kDa	<i>Apis mellifera</i> (Western honey bee)/Insecta	Ga-07	66547450	127/2(1)	3	60.375	54.62	Yes	[9, 64]
Similar to predicted protein (heat shock protein 83 kDa)	<i>Hydra magnipapillata</i> (Hydra)/Cnidaria	Ga-03	221124690	73/2(2)	2	94.208	104.60		
Unnamed protein product (GroEL-like type I chaperonin)	<i>Mus musculus</i> (house mouse)/Vertebrata	Ga-07	51452	127/2(1)	3	58.833	54.62		

Table 2. Continued

Protein name	Species/Taxonomy	Band no.	GI no.	MS/ mps(p) ^a	Sequence coverage (%)	Predicted MW (kDa)	Observed MW (kDa)	Found with LBs in other organisms	Reference(s)
DNA repair and metabolism									
ATP-dependent exoDNase (β subunit)	<i>Erythro bacter litoralis</i> HTCC2594/ Proteobacteria	Ga-03	85373841	60/2(2)	1	125.666	104.60		
Breast cancer 1 (BRCA1)	<i>Macropus irma</i> (wallaby)/Vertebrata	Ga-06	223369569	56/2(2)	3	85.417	58.20	Yes	[67]
Histone family protein	<i>Prevotella oralis</i> ATCC 33269 / Bacteria	Ga-08	315611484	65/2(2)	15	15.621	51.00	Yes	[9, 64]
Histone H2A	<i>Chironomus thummi</i> (midge)/Insecta	Ga-07	122001	111/2(2)	41	13.415	54.62	Yes	[9, 64]
Transporter									
Mitochondrial carrier protein (ADP/ATP transporter)	<i>N. vectensis</i> (sea anemone)/Cnidaria	Ga-10	156401103	593/12(8)	28	33.237	32.50		
Sarco/ER calcium ATPase	<i>Bombyx mori</i> (domesticated silkworm)/Insecta	Ga-07	256773186	268/8(8)	10	112.582	54.62		
Similar to arsA arsenite transporter (anion-transporting ATPase)	<i>Ciona intestinalis</i> (vase tunicate)/Chordata	Ga-07	198427247	88/3(2)	1	126.935	54.62		
Cytoskeleton and Intracellular trafficking									
Actin	<i>Galaxea fascicularis</i> (coral)/Cnidaria	Ga-09	26522784	662/26(11)	39	41.689	46.01	Yes	[5, 9, 19, 20, 68]
α -Tubulin	<i>Paracentrotus lividus</i> (purple sea urchin)/ Metazoa	Ga-07	135400	135/2(2)	6	50.177	54.62	Yes	[5, 12, 17, 20]
β -Tubulin	<i>Haliclona rubens</i> (sponge)/Metazoa	Ga-06	32967414	68/7(7)	21	43.146	58.20	Yes	[5, 12, 17, 20]
GA25794 (myosin and kinesin motor domain)	<i>Drosophila pseudoobscura</i> (fruit fly)/ Insecta	Ga-07	198474044	1127/ 54(35)	35	248.543	54.62	Yes	[20, 52]
Predicted protein (stomatin)	<i>N. vectensis</i> (sea anemone)/Cnidaria	Ga-10	156390662	132/3(3)	12	31.238	32.50	Yes	[19]
Tropomyosin	<i>A. aegypti</i> (mosquito)/Insecta	Ga-07	157131823	133/6(5)	19	30.982	54.62		
Troponin I (isoform 6a2)	<i>Ap. mellifera</i> (Western honey bee)/Insecta	Ga-07	78101804	50/2(2)	8	25.183	54.62		
Unknown (actin)	<i>Glycine max</i> (soybean)/Streptophyta	Ga-08	255645644	56/2(2)	7	41.508	51.00	Yes	[5, 9, 19, 20, 68]
Unnamed protein product (α actinin)	<i>D. melanogaster</i> (fruit fly)/Insecta	Ga-07	8186	87/2(2)	2	104.05	54.62	Yes	[52]
Protein biosynthesis and metabolism									
Cysteine desulfurase, mitochondrial precursor	<i>Salmo salar</i> (Atlantic salmon)/Vertebrata	Ga-07	209149601	82/2(1)	3	49.748	54.62		
Elongation factor 1 α	<i>Cinara etsuhoel</i> /Insecta	Ga-10	5670229	75/2(2)	8	30.083	32.50	Yes	[5, 9, 52]
Predicted protein (EF-Tu subfamily)	<i>N. vectensis</i> (sea anemone)/Cnidaria	Ga-09	156380782	122/2(2)	6	43.961	46.01	Yes	[59]
Miscellaneous									
Carbonic anhydrase 2	<i>Bos taurus</i> (cattle)/Vertebrata	Ga-10	30466252	50/2(2)	7	29.096	32.50		
Formate dehydrogenase (α subunit)	Marine γ proteobacterium HTCC2207/ Proteobacteria	Ga-02	90416712	50/2(2)	2	103.602	191.23		
Glutamate synthase (NADPH)	<i>Methanocella paludicola</i> SANAe/Archae	Ga-07	282163659	57/2(2)	5	50.901	54.62		
Multi-sensor hybrid histidine kinase	<i>Candidatus Koribacter versatilis</i> Ellin345 (Acidobacteria)/Bacteria	Ga-02	94969524	65/2(2)	1	129.81	191.23		

a) MS/mps(p): MOWSE score/number of total matched peptides (numbers of different matched peptides). For criteria for positive protein identification, see Section 2.

stability [51], and are involved in lipolysis, FA-binding, membrane targeting, and lipid trafficking [2]. Nevertheless, members of the PAT protein family were not identified in SGC LBs (Table 2) or yeast lipid droplets [7]. Furthermore, small GTPase proteins (e.g. Rab and ARF) occasionally found in animal lipid droplets [51] were also absent in coral LBs. These absences may suggest that LBs in this marine endosymbiosis differ from lipid droplets in other cell species in terms of their biogenesis and function.

It is also striking to note that, among the 42 identified proteins, there was only one of dinoflagellate origins, most closely resembling a putative actin from *Streptohyta* (Table 2). The dominance of proteins of presumed host origin may indicate a dominant role of the host in LB biogenesis. On the other hand, prior work found that the majority of the lipids within the LBs are of *Symbiodinium* origin [27], suggesting that both members of this endosymbiosis are involved in LB biogenesis and function.

The differences in the protein composition of coral SGC LBs compared with those of other species may help to shed light on their unique morphological characteristics, described in detail below, as well as further the understanding of their role in this environmentally important marine endosymbiosis. This link between the LB ultrastructure and proteome is discussed in the following sections.

3.2.1 General in situ morphology of LBs

In comparison with lipid droplets of other eukaryotic cells, there are several unique morphological characteristics of LBs in this coral–dinoflagellate endosymbiosis (Fig. 5). First, they exhibit high electron density upon transmission electron microscopy (TEM) examination (see “LB” in Fig. 5A), suggesting that the major core components are different from those of lipid droplets in other eukaryotic cells. For example, numbers of unsaturated bonds in TGs resulting from feeding cells with FAs have been shown to determine the TEM electron density of lipid droplets [54]. Based on the high reactivity of osmium tetroxide with unsaturated FAs, an increase in the electron density of the lipid droplets as

examined by quantitative TEM imaging analysis was observed when more unsaturated FAs were fed to both fibroblasts and adipocytes [54]. The electron density of lipid droplets varies across cell types, ranging from low (e.g. adipocytes [54]) to high (e.g. leukocytes [5]). The LBs in *E. glabrescens* are more similar to the latter in that they are characterized by a high electron density suggestive of a high level of unsaturated TGs. This is also confirmed that, among other lipids, TGs are most abundant in both weight concentration ($87.21 \pm 10.20 \mu\text{g}/\mu\text{g}$ protein) and molecular number ($\sim 6.51 \times 10^{16}$ molecules/ μg protein) in coral LBs (Table 1).

As a second notable characteristic, sections of the LBs exhibited rectangular, electron-transparent inclusions, measuring 1–2 μm in length and 25–30 nm in width (see blank arrows in Fig. 5A and B). The occurrence of these inclusions varied in the LBs examined and covered an average area between 1.87 and 30.88% of the LB TEM section. The nature of these inclusions remains to be elucidated. However, they may represent regions containing lipid species without unsaturated bonds, or not reactive with osmium tetroxide such as sterols and WEs [1, 54, 55]. As previously shown, the electron density of cholesterol-rich lipid droplets was generally low [54]. Similar inclusions have also been found in lipid vesicles in both epiderm and gastroderm of corals such as *Acropora acuminata* [26], *Astrangia danae*, *Porites porites* [56], and larvae of *Pocillopora damicornis* [57]. Based on the ultrastructural appearance, these inclusions were concluded to contain WEs, and were associated with mucus-producing cells [26]. Nonetheless, the chemical nature of these LB inclusions in the present study requires future investigation. In some cases, ultrastructural examination showed that they were connected with adjacent *Symbiodinium* via numerous fibrous or membranous structures (Fig. 5B). As shown in the magnified inset (Fig. 5C), there was a very close attachment of these structures with the *Symbiodinium* (see the blank arrows). These structures further extend into the site of the inclusions in the LBs (see the filled arrows).

Third, the LBs were in close spatial proximity to mitochondria, ER, and Golgi apparatus. As shown in Fig. 5A, mitochondria were commonly observed around the LB. The ER (both smooth ER (SER) and rough ER (RER)) was another significant organelle in close contact with the LBs. Whether these close proximity indicates a functional relationship between LBs and cellular organelles, or it is just resulted from a space limitation in the SGC due to the presence of bulky symbionts (Fig. 2E) remains to be elucidated.

3.2.2 Biological function of LBs

Based on the number of identified proteins in different functional categories (Fig. 4), LBs are implicated to have four major biological functions (Fig. 4 and Table 2) in the following prioritized order; (i) lipid and energy metabolism (12 identified proteins out of 42), (ii) cytoskeleton formation

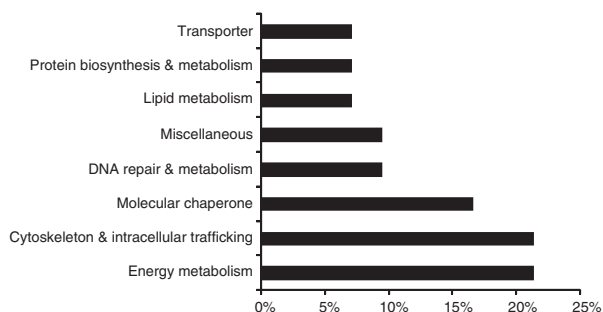


Figure 4. Functional categories of the identified, LB-associated proteins.

and intracellular trafficking (9 out of 42), (iii) stress response/molecular modification (7 chaperone proteins out of 42), and (iv) development (4 DNA repair and metabolism proteins out of 42).

3.2.2.1 Role in lipid and energy metabolism

The defining characteristic of LBs is their high concentration of lipids, which was used as one of the criteria for the validation of LB purification in the present study (Fig. 3A). As summarized in Table 1, LBs contained seven lipid species, including TG, sterols, WE, lysophosphatidylcholine, FA, PC, and PE in the prioritized order of molecular number per microgram LB protein. Similar to lipid droplets in other eukaryotic cells, TGs are most abundant [44, 54]. However, it is surprising to note that other lipid composition in coral LBs is different from those of lipid droplets in other eukaryotic cells. Mainly, steryl ester (or cholesterol ester), a common lipid in mammalian cells [44], was not detected in the gastrodermal LBs. Instead, sterols are

significantly enriched in both weight concentration ($6.92 \pm 0.87 \mu\text{g}/\mu\text{g}$ protein) and molecular number (1.08×10^{16} molecules/ μg protein) in the gastrodermal LBs (Table 1). Moreover, WEs, which were not found in lipid droplets of mammalian cells [44], were present in the gastrodermal LBs with a weight concentration of $7.31 \pm 0.55 \mu\text{g}$ ($\sim 9.15 \times 10^{15}$ molecules) per microgram protein. Here, the presence of WE and absence of steryl ester in coral LBs are similar to lipid droplets in plants [44]. This suggests that *Symbiodinium* could be the manufacturer of the WE that ultimately migrates to the gastrodermal LBs. Molecular numbers of FAs and other phospholipids ranged from $\sim 2.67 \times 10^{14}$ to 3.18×10^{15} , and their enrichments were lower than those of WE, TG, and sterols (Table 1). Whether this may be resulted from the nonspecific removal by the Tween-20 washing remains to be elucidated.

The MS examination showed that there were three LB-associated proteins involved in lipid metabolism, including phospholipase D, *S*-adenosyl-L-homocysteine hydrolase and acetyl-CoA acetyltransferase (Table 2). Phospholipase D (PLD) hydrolyzes the phosphodiester bond of the glycerolipid PC, resulting in the production of phosphatidic acid and free choline [58]. Phosphatidic acid is widely considered to be the intracellular lipid mediator of many of the biological functions attributed to Phospholipase D [58]. In eukaryotes, *S*-adenosyl-L-homocysteine hydrolase offers a single way for the degradation of *S*-adenosyl-L-homocysteine, a product and potent competitive inhibitor of *S*-adenosyl-L-methionine (AdoMet)-dependent methyltransferases, and is involved in homeostasis of cellular PC [59]. Acetyl-CoA acetyltransferase is an enzyme which converts two units of acetyl-CoA to acetoacetyl CoA in the mevalonate pathway [9]. It has key roles in many vital biochemical pathways, including the β -oxidation pathway of FA degradation and various biosynthetic pathways [9]. The identification of these three enzymes indicates that there are active lipid catabolic processes occurring on or within LBs. LBs have been proposed to store neutral lipids as an energy source [39], and this hypothesis is supported by the proteomic data (Table 2), which, in addition to the three lipid metabolism proteins, unveiled nine additional enzymes involved in various energy metabolism pathways, including ATP synthesis, glycolysis, and the tricarboxylic acid cycle. These results suggest that LBs may not only serve as lipid repositories, but may also represent a dynamic nexus of lipid metabolism.

TGs are synthesized by the action of acyl CoA:diacylglycerol acyltransferase (DGAT, EC 2.3.1.20) with diacylglycerol and fatty acyl CoAs as substrates [44]. However, both DGAT and diacylglycerol for TG synthesis were not identified in coral LBs. It may indicate that TGs are not synthesized in situ in LBs. Future investigations to examine the distribution of DGAT should provide critical insight to understand how TGs are accumulated in coral LBs.

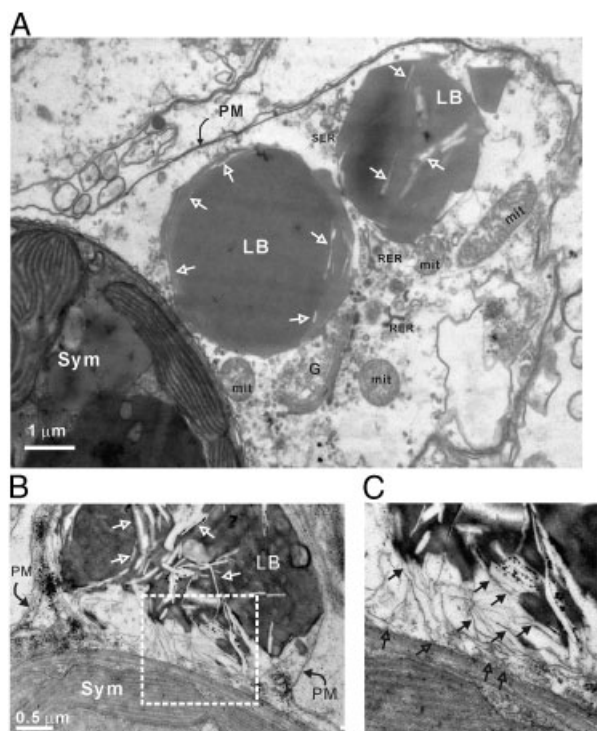


Figure 5. In situ morphology of coral LBs. LB ultrastructure was examined by TEM in the gastroderm of the coral tentacle. (A) The distribution of two LBs inside a SGC. PM, plasma membrane and Sym, *Symbiodinium*. Smooth or rough ER (SER, RER, respectively), mitochondria (mit) and Golgi apparatus (G) were often found adjacent to LBs. Furthermore, long, narrow inclusions with low electron density (arrows) inside individual LBs were repeatedly observed, an example of which is demonstrated in (B). (B) An example of a LB with numerous fibrous structures connecting to the adjacent *Symbiodinium*. The selected region is magnified in (C), showing that these fibrous structures originated from the endosymbiont's surface (see blank arrows), and extended into the LB (see filled arrows).

3.2.2.2 Role of the cytoskeleton and intracellular trafficking

The functional category with the second greatest number of proteins identified in LBs (9 out of the 42 (21%); Table 2 and Fig. 4) is “cytoskeleton and intracellular trafficking.” Two actins (GI No. 26522784 and 255645644), four actin-binding proteins (GA25794, tropomyosin, troponin I isoform 6a2 and α -actinin) and two tubulin species (β -tubulin and tubulin α -1 chain) were identified, indicating the important role of the cytoskeleton in LBs. In fact, the Western blot examination also showed that there was specific actin species in the purified LBs (Fig. 3B, “Buoyant detergent-washed LB” fraction). The nature of this actin requires further investigation, as it is unclear whether it is truly associated with the LBs, or a contaminant difficult to be removed. In a previous study, cytoskeletal proteins have been identified as LB components, and β -actin has been shown to form a cage around lipid droplets in rat adrenocortical cells and adipocytes [60]. Attachment sites of tubulin on the LB surface are visible as spikes, and nocodazole treatment results in diffuse tubulin, which affects vesicle distribution [19].

Lipid droplets have been shown to migrate along cytoskeletal elements during growth and disintegration [61]. Their movement may also promote nutrient delivery from one location to another. For example, in *Drosophila*, cytoplasmic streaming delivers droplets from their site of synthesis in nurse cells to the oocyte and thus ultimately to the embryo [9, 62]. The elucidation of LB movement during the coral-*Symbiodinium* endosymbiosis remains a challenge due to the bulky dinoflagellate(s) that occupy almost all of the space within the host gastrodermal cell. Their presence could, then, inhibit the observation of motion of LBs by microscopic examination.

Lipid droplets have been shown to be active and dynamic cellular organelles that govern lipid homeostasis and intracellular trafficking in a variety of mammalian cells [52]. They have been shown to regulate lipid trafficking by intercommunication with the Golgi apparatus, ER, numerous intracellular vesicles, and the plasma membrane. Many proteins involved in intracellular trafficking have been identified on lipid droplets, including ARF, Rab, Rho, and their regulatory proteins [52]. Nevertheless, in the present study, such intracellular trafficking proteins were undetected in the gastrodermal LBs (Table 2). In particular, the absence of ARF was also confirmed by the Western blot examination (Fig. 3B). The association of small GTPase proteins with lipid droplets is variable and cell-type specific (for review, see [63]). In fact, both Rho and ARF proteins were less frequently observed in lipid droplets, especially of yeast and *Drosophila* [63]. However, a cnidarian homolog of stomatin was identified in the gastrodermal LBs. Stomatin has been shown to associate with LBs of MDCK cells [19]. Blocking of protein synthesis leads to the redistribution of stomatin from LBs to lysosomes, indicating the critical role of stomatin in regulating the vesicular trafficking of LBs with other cellular compartments [19].

3.2.2.3 Role in the stress response and molecular modification

Seven molecular chaperones, including DnaK, HSP70, HSP83, HSP90, and three others, were identified in coral LBs, with all likely to be of host origin based on homology searches (Table 2). Except for HSP83 and the GroEL-like type I chaperonin, the other chaperones have been identified in LBs of other cell types [5, 12, 15, 17, 19, 64]. For instance, it was proposed that enhanced formation of lipid droplets in rat pheochromocytoma cells (PC12) could be a response to nanomaterial-induced stresses [65]. In this study, the relatively large number of coral LB molecular chaperones identified by MS could indicate that LBs may be a site of protein modification in response to diel protein denaturation resulting from reactive oxygen species production during photosynthesis *in hospice* [66].

3.2.2.4 Role in development

Among the 42 identified proteins, four (10%) are nuclear proteins, including the ATP-dependent exoDNAse β subunit, BRCA1, histone family protein, and histone H2A (Table 2). The presence of histones in lipid droplets is intriguing and has only been observed in human leukocytes (U937 cells [5]) and invertebrate embryos (*Drosophila* [9, 13]). In the latter, using biochemical and real-time imaging, it was found that lipid droplets serve as transient storage depots for proteins during embryonic development [9]. Almost 50% of known embryonic histones are physically attached to lipid droplets during oogenesis in early embryonic development. Accumulated histones are then transferred from the lipid droplets to the nuclei as development proceeds. As typical histones have not been detected in *Symbiodinium* [31], the histone H2A is likely of host origin and implicates a potential role of LBs in the regulation of coral development.

3.3 LB biogenesis

The mechanism of host LB assembly in cnidarians remains completely unknown [27]. Previous studies have indicated that lipid droplets originate from the ER in a variety of eukaryotic cells (for review, see [3, 4]), in which neutral lipids (including TGs and cholesterol esters) are synthesized between leaflets of the ER membrane and later bud off to form independent lipid droplets [15, 59]. The presence of ER-like membranes around and within LBs has been reported in activated leukocytes, such as human neutrophils and eosinophils, when LB formation was enhanced [5]. As a consequence, lipid droplets were enclosed in a phospholipid monolayer derived from the ER. However, the presence of a monolayer phospholipid membrane around the LB was not specifically examined in the present study. SER and/or RER were often observed to distribute around the LBs (Figs. 5A). It is also intriguing to note that the SER was seen to enclose individual LBs in

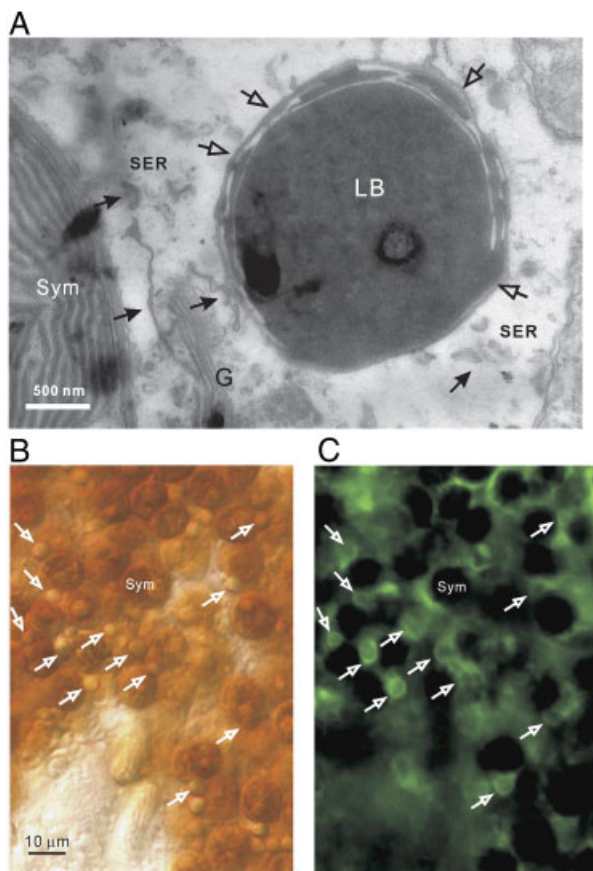


Figure 6. Association of the ER with LBs. (A) The close distribution of the SER (see filled arrows) with the LBs. This particular LB was also surrounded by a SER (see blank arrows). (B and C) The distribution of LBs and ER in live gastrodermal tissue. (B) The DIC image of the gastrodermis, indicating the LB distribution (see blank arrows); (C) The ER labeling in the same tissue by ER-Tracker™ Green. Sym, the *Symbiodinium*.

some cases (blank arrows of Fig. 6A). The distribution of the ER around LBs was further confirmed *in vivo* with the ER-Tracker Green probe. As indicated by arrows in Fig. 6B and C, the fluorescent labeling displayed a characteristic, ring-like distribution over the surface of the LBs. The close relationship of the ER with the LBs was further demonstrated by the identification of the ER-specific chaperone Bip (GRP 78, Table 2). Nevertheless, the mere observation of host ER around the LB surface is not enough to provide a mechanism for LB biogenesis, and hence future research will attempt to unveil such a mechanism in this coral-dinoflagellate endosymbiosis.

4 Concluding remarks

LBs are likely to be important pivotal organelles in coral-*Symbiodinium* endosymbioses, and their biogenesis and cellular function should be the targets for future investigation.

The suite of proteins found to be associated with LBs purified from SGCs indicates that LBs are involved in an array of cellular processes. In combination with morphological investigations of LBs using confocal and TEM, the present study clearly shows that both the morphology and the molecular composition (proteins and lipids) of LBs are significantly different from those of other eukaryotic cells. These differences may stem from the endosymbiotic nature of this association in which it is likely that both the host and endosymbionts play a role in the regulation of LB biogenesis and function.

This work was supported by grants from the National Science Council of Taiwan (NSC 98-2311-B-291-001-MY3; NSC 98-2311-291-002-MY3 to SEP and CSC) and by intramural funding from the National Museum of Marine Biology and Aquarium (99200311; 99200313). The authors thank the Center for Resources, Research and Development of Kaohsiung Medical University for their instrumental support of this work. Finally, the authors thank Professor Chung-Hsiung Wang for his insight on lipid body morphology during the initial stages of this study.

The authors have declared no conflict of interest.

5 References

- [1] Waltermann, M., Steinbuchel, A., Neutral lipid bodies in prokaryotes: recent insights into structure, formation, and relationship to eukaryotic lipid droplets. *J. Bacteriol.* 2005, **187**, 3607–3619.
- [2] Olofsson, S. O., Bostrom, P., Andersson, L., Rutberg, M. et al., Lipid droplets as dynamic organelles connecting storage and efflux of lipids. *Biochim. Biophys. Acta* 2009, **1791**, 448–458.
- [3] Ohsaki, Y., Cheng, J., Suzuki, M., Fujita, A., Fujimoto, T., Lipid droplets are arrested in the ER membrane by tight binding of lipidated apolipoprotein B-100. *J. Cell Sci.* 2008, **121**, 2415–2422.
- [4] Robenek, H., Hofnagel, O., Buers, I., Robenek, M. J. et al., Adipophilin-enriched domains in the ER membrane are sites of lipid droplet biogenesis. *J. Cell Sci.* 2006, **119**, 4215–4224.
- [5] Wan, H. C., Melo, R. C. N., Jin, Z., Dvorak, A. M., Weller, P. F., Roles and origins of leukocyte lipid bodies: proteomic and ultrastructural studies. *FASEB J.* 2007, **21**, 167–178.
- [6] Tauchi-Sato, K., Ozeki, K. S., Honjou, T., Taguchi, R., Fujimoto, T., The surface of lipid droplets is a phospholipid monolayer with a unique fatty acid composition. *J. Biol. Chem.* 2002, **277**, 44507–44512.
- [7] Athenstaedt, K., Zweytick, D., Jandrozitz, A., Kohlwein, S. D., Daum, G., Identification and characterization of major lipid particle proteins of the yeast *Saccharomyces cerevisiae*. *J. Bacteriol.* 1999, **181**, 6441–6448.
- [8] Fujimoto, T., Itabe, H., Sakai, J., Makita, M. et al., Identification of major proteins in the lipid droplet-enriched frac-

- tion isolated from the human hepatocyte cell line HuH7. *Biochim. Biophys. Acta* 2004, 1644, 47–59.
- [9] Cermelli, S., Guo, Y., Gross, S. P., Welte, M. A., The lipid-droplet proteome reveals that droplets are a protein-storage depot. *Curr. Biol.* 2006, 16, 1783–1795.
- [10] Londos, C., Brasaemle, D. L., Schultz, C. J., Segrest, J. P., Kimmel, A. R., Perilipins, ADRP, and other proteins that associate with intracellular neutral lipid droplets in animal cells. *Semin. Cell Dev. Biol.* 1999, 10, 51–58.
- [11] Mirua, S., Gan, J. W., Brzostowski, J., Parisi, M. J. et al., Functional conservation for lipid storage droplet association among Perilipin, ADRP, and TIP47 (PAT)-related proteins in mammals, *Drosophila*, and *Dictyostelium*. *J. Biol. Chem.* 2002, 277, 32253–32257.
- [12] Brasaemle, D. L., Dolios, G., Shaprio, L., Wang, R., Proteomic analysis of proteins associated with lipid droplets of basal and lipolytically stimulated 3T3-L1 adipocytes. *J. Biol. Chem.* 2004, 279, 46835–46842.
- [13] Welte, M. A., Proteins under new management: lipid droplets delivery. *Trends Cell Biol.* 2007, 17, 363–369.
- [14] Duncan, R. E., Ahmadian, M., Jaworski, K., Sarkadi-Nagy, E., Sul, H. S., Regulation of lipolysis in adipocytes. *Annu. Rev. Nutr.* 2007, 27, 79–101.
- [15] Prattes, S., Horl, G., Hammer, A., Blaschitz, A. et al., Intracellular distribution and mobilization of unesterified cholesterol in adipocytes: triglyceride droplets are surrounded by cholesterol-rich ER-like surface layer structures. *J. Cell Sci.* 2000, 113, 2977–2987.
- [16] Maxfield, F. R., Tabas, I., Role of cholesterol and lipid organization in disease. *Nature* 2005, 438, 612–621.
- [17] Liu, P., Ying, Y., Zhao, Y., Mundy, D. I. et al., Chinese hamster ovary K2 cell lipid droplets appear to be metabolic organelles involved in membrane traffic. *J. Biol. Chem.* 2004, 279, 3787–3792.
- [18] Ozeki, S., Cheng, J., Tsuchi-Sato, K., Hatano, N. et al., Rab18 localizes to lipid droplets and induces their close apposition to the endoplasmic reticulum-derived membrane. *J. Cell Sci.* 2005, 118, 2601–2611.
- [19] Umlauf, E., Császár, E., Moertelmaier, M., Schuetz, G. J. et al., Association of stomatin with lipid bodies. *J. Biol. Chem.* 2004, 279, 23699–23709.
- [20] Turro, S., Ingelmo-Torres, M., Estanyol, J. M., Tebar, F. et al., Identification and characterization of associated with lipid droplet protein 1: a novel membrane-associated protein that resides on hepatic lipid droplets. *Traffic* 2006, 7, 1254–1269.
- [21] Wu, C. C., Howell, K. E., Neville, M. C., Yates, J. R., McManaman, J. L., Proteomics reveal a link between the endoplasmic reticulum and lipid secretory mechanisms in mammary epithelial cells. *Electrophoresis* 2000, 21, 3470–3482.
- [22] Pol, A., Martin, S., Fernandez, M. A., Ferguson, C. et al., Dynamic and regulated association of caveolin with lipid bodies: modulation of lipid body motility and function by a dominant negative mutant. *Mol. Biol. Cell* 2004, 15, 99–110.
- [23] Targett-Adams, P., Chambers, D., Gledhill, S., Hope, R. G. et al., Live cell analysis and targeting of the lipid droplet-binding adipocyte differentiation-related protein. *J. Biol. Chem.* 2003, 278, 15998–16007.
- [24] Peng, S. E., Wang, Y. B., Wang, L. H., Chen, W. N. U. et al., Proteomic analysis of symbiosome membranes in cnidarian-dinoflagellate endosymbiosis. *Proteomics* 2010, 10, 1002–1016.
- [25] Patton, J. S., Burris, J. E., Lipid synthesis and exclusion by freshly isolated zooxanthellae (symbiotic algae). *Mar. Biol.* 1983, 75, 131–136.
- [26] Crossland, C. J., Barnes, D. J., Borowitzka, M. A., Diurnal lipid and mucus production in the staghorn coral *Acropora acuminata*. *Mar. Biol.* 1980, 60, 81–90.
- [27] Luo, Y. J., Wang, L. H., Chen, W. N. U., Peng, S. E. et al., Ratiometric imaging of gastrodermal lipid bodies in coral-dinoflagellate endosymbiosis. *Coral Reefs* 2009, 28, 289–301.
- [28] Chen, C. S., Lin, H. P., Yeh, C. C., Fang, L. S., Use of a fluorescent membrane probe to identify zooxanthellae in hospite among dissociated endoderm cell culture from coral. *Protoplasma* 2005, 226, 175–179.
- [29] Barthel, L. K., Raymond, P. A., Improved method for obtaining 3-microns cryosections for immunocytochemistry. *J. Histochem. Cytochem.* 1990, 38, 1383–1388.
- [30] Greenspan, P., Mayer, E. P., Fowler, S. D., Nile red: a selective fluorescent stain for intracellular lipid droplets. *J. Cell Biol.* 1985, 100, 965–973.
- [31] Peng, S. E., Luo, Y. J., Huang, H. J., Lee, I. T. et al., Isolation of tissue layers in hermatypic corals by N-acetylcysteine: morphological and proteomic examinations. *Coral Reefs* 2008, 27, 133–142.
- [32] Bligh, E. G., Dyer, W. J., A rapid method for total lipid extraction and purification. *Can. J. Biochem. Physiol.* 1959, 37, 911–917.
- [33] Oku, H., Yamashiro, H., Onaga, K., Lipid biosynthesis from [¹⁴C]-glucose in the coral *Montipora digitata*. *Fish. Sci.* 2003, 69, 625–631.
- [34] Fuchs, B., Schiller, J., Sub, R., Schurenberg, M. et al., A direct and simple method of coupling matrix-assisted laser desorption and ionization time-of-flight mass spectrometry (MALDI-TOF MS) to thin-layer chromatography (TLC) for the analysis of phospholipids from egg yolk. *Anal. Bioanal. Chem.* 2007, 389, 827–834.
- [35] Abe, A., Modification of the Coomassie brilliant blue staining method for sphingolipid synthesis inhibitors on silica gel thin-layer plate. *Anal. Biochem.* 1998, 258, 149–150.
- [36] Mastro, R., Hall, M., Protein delipidation and precipitation by tri-n-butylphosphate, acetone, and methanol treatment for isoelectric focusing and two dimensional gel electrophoresis. *Anal. Biochem.* 1999, 273, 313–315.
- [37] Laemmli, U. K., Cleavage of structural proteins during the assembly of the head of bacteriophage T4. *Nature* 1970, 227, 680–685.
- [38] Towbin, H., Staehelin, T., Gordon, J., Electrophoretic transfer of proteins from polyacrylamide gels to nitrocellulose sheets: procedure and some applications. *Proc. Nat. Acad. Sci. USA* 1979, 76, 4350–4354.

- [39] Kellog, R. B., Patton, J. S., Lipid droplets, medium of energy exchange in the symbiotic anemone *Condylactis gigantea*: a model coral polyp. *Mar. Biol.* 1983, *75*, 137–149.
- [40] Muscatine, L., Gates, R. D., LaFontaine, I., Do symbiotic dinoflagellates secrete lipid droplets? *Limnol. Oceanogr.* 1994, *39*, 925–929.
- [41] Fujimoto, T., Ohsaki, Y., Cytoplasmic lipid droplets: rediscovery of an old structure as a unique platform. *Ann. NY Acad. Sci.* 2006, *1086*, 104–115.
- [42] Vercauteren, F. G. G., Arckens, L., Quirion, R., Application and current challenges of proteomic approaches, focusing on two-dimensional electrophoresis. *Amino Acids* 2007, *33*, 405–414.
- [43] Afdhal, N. H., Cao, X., Bansil, R., Hong, Z. et al., Interaction of mucin with cholesterol enriched vesicles: role of mucin structural domains. *Biomacromolecules* 2004, *5*, 269–275.
- [44] Zweytick, D., Athenstaedt, K., Daum, G., Intracellular lipid particles of eukaryotic cells. *Biochim. Biophys. Acta* 2000, *1469*, 101–120.
- [45] Harland, A. B., Fixer, L. M., Davies, P. S., Anderson, R. A., Distribution of lipids between the zooxanthellae and animal compartment in the symbiotic sea anemone *Anemonia viridis*: wax ester, triglycerides, and fatty acids. *Mar. Biol.* 1991, *110*, 13–19.
- [46] Sang, A., ARF1 regulatory factors and COPI vesicle formation. *Curr. Opin. Cell Biol.* 2002, *14*, 423–427.
- [47] Cavenagh, M. M., Whitney, J. A., Carroll, K., Zhang, C.-J. et al., Intracellular distribution of Arf proteins in mammalian cells. *J. Biol. Chem.* 1996, *271*, 21767–21774.
- [48] Kametaka, S., Sawada, N., Bonifacino, J. S., Waguri, S., Functional characterization of protein-sorting machineries at the trans-Golgi network in *Drosophila melanogaster*. *J. Cell Sci.* 2010, *123*, 460–471.
- [49] Tzen, J. T. C., Peng, C.-C., Cheng, D.-J., Chen, E. C. F. et al., A new method for seed oil body purification and examination of oil body integrity following germination. *J. Biochem.* 1997, *121*, 762–768.
- [50] Schick, M. J., Effect of temperature on the critical micelle concentration of nonionic detergents. Thermodynamics of micelle formation. *J. Phys. Chem.* 1963, *67*, 1796–1799.
- [51] Goodman, J. M., The gregarious lipid droplets. *J. Biol. Chem.* 2008, *283*, 28005–28009.
- [52] Bartz, R., Zehmer, J. K., Zhu, M., Chen, Y. et al., Dynamic activity of lipid droplets: protein phosphorylation and GTP-mediated protein translocation. *J. Proteome Res.* 2007, *6*, 3256–3265.
- [53] Tzen, J. T. C., Huang, A. H. C., Surface structure and properties of plant seed oil bodies. *J. Cell Biol.* 1992, *117*, 327–335.
- [54] Cheng, J., Fujita, A., Ohsaki, Y., Quantitative electron microscopy shows uniform incorporation of triglycerides into existing lipid droplets. *Histochem. Cell Biol.* 2009, *132*, 281–291.
- [55] Ishie, T., Tani, A., Takabe, K., Kawasaki, K. et al., Wax ester production from n-alkanes by *Actinetobacter* sp. strain M-1: ultrastructure of cellular inclusions and role of acyl coenzyme A reductase. *Appl. Environ. Microbiol.* 2002, *68*, 1192–1195.
- [56] Hayes, R. L., Goreau, N. I., Intracellular crystal-bearing vesicles in the epidermis of scleractinian corals, *Astrangia danae* (Agassiz) and *Porites porites* (Pallas). *Biol. Bull.* 1977, *152*, 26–40.
- [57] Vandermeulen, J. H., Studies on reef corals, II. Fine structure of planktonic planula larva of *Pocillopora damicornis*, with emphasis on the aboral epidermis. *Mar. Biol.* 1974, *27*, 239–249.
- [58] Jenkin, G. M., Frohman, M. A., Phospholipase D: a lipid centric view. *Cell Mol. Life Sci.* 2005, *62*, 2305–2316.
- [59] Low, K. L., Shui, G., Natter, K., Yeo, W. K. et al., Lipid droplet-associated proteins are involved in the biosynthesis and hydrolysis of triacylglycerol in *Mycobacterium bovis bacillus* Calmette-Guerin. *J. Biol. Chem.* 2010, *285*, 21662–21670.
- [60] Fong, T. H., Wu, C. H., Liao, E. W., Chang, C. Y. et al., Association of globular-actin with intracellular lipid droplets in rat adrenocortical cells and adipocytes. *Biochem. Biophys. Res. Comm.* 2001, *289*, 1168–1174.
- [61] Welte, M. A., Fat on the move: intracellular motion of lipid droplets. *Biochim. Soc. Trans.* 2009, *37*, 991–996.
- [62] Gross, S. P., Guo, Y., Martinez, J. E., Welte, M. A., A determinant for directionality of organelle transport in *Drosophila* embryo. *Curr. Biol.* 2003, *13*, 1660–1668.
- [63] Hodges, B. D. M., Wu, C. C., Proteomic insights into an expanded cellular role for cytoplasmic lipid droplets. *J. Lipid Res.* 2010, *51*, 262–273.
- [64] Sato, S., Fukasawa, M., Yamakawa, Y., Natsume, T. et al., Proteomic profiling of lipid droplet proteins in hepatoma cell lines expressing hepatitis C virus core protein. *J. Biochem. (Tokyo)* 2006, *139*, 921–930.
- [65] Khatchadourian, A., Maysinger, D., Lipid droplets: their role in nanoparticle-induced oxidative stress. *Mol. Pharmaceutics* 2009, *6*, 1125–1137.
- [66] Richier, S., Rodriguez-Lanetty, M., Schnitzler, C., Weis, V. M., Response of the symbiotic cnidarian *Anthopleura elegantissima* transcriptome to temperature and UV increase. *Comp. Biochem. Physiol.* 2008, *D3*, 283–289.
- [67] Spitsberg, V. L., Bovine milk fat globule membrane as a potential nutraceutical. *J. Dairy Sci.* 2005, *88*, 2289–2294.
- [68] Fong, T. H., Wu, C. H., Liao, E. W., Chang, C. Y. et al., Association of globular beta-actin with intracellular lipid droplets in rat adrenocortical cells and adipocytes. *Biochem. Biophys. Res. Comm.* 2001, *289*, 1168–1174.